Xi'an Shiyou Daxue Xuebao (Ziran Kexue Ban)/
Journal of Xi'an Shiyou University, Natural Sciences Edition
ISSN: 1673-064X
E-Publication: Online Open Access
Vol: 67 Issue 04 | 2024
DOI: 10.5281/zenodo.11063869

POLYMERIC NANOPARTICLE FORMULATION OF LORNOXICAM WITH ENHANCED AQUEOUS SOLUBILITY AND IMPROVED ANTI-INFLAMMATORY EFFECT

RABIA NOOR *
Department of Pharmaceutics, Faculty of Pharmacy and Pharmaceutical Sciences, University of Karachi, Karachi, Pakistan. *Corresponding Author Email: rabianoor@student.ku.edu.pk

SYED MUHAMMAD FARID HASAN
Department of Pharmaceutics, Faculty of Pharmacy and Pharmaceutical Sciences, University of Karachi, Karachi, Pakistan.

SHAZIA HAIDER
Department of Pharmaceutical Chemistry, Faculty of Pharmacy and Pharmaceutical Sciences, University of Karachi, Karachi, Pakistan. Email: shazia.haider@uok.edu.pk

FAHEEMA SIDDIQUI
Department of Pharmacology, Dow College of Pharmacy, Dow University of Health Sciences, Karachi, Pakistan.

SHAHNAZ USMAN
Department of Pharmaceutics, RAK College of Pharmacy, RAK Medical and Health Science University, Ras Al Khaimah, UAE.

SADAF NAZ
Department of Pharmaceutical Chemistry, Faculty of Pharmacy and Pharmaceutical Sciences, University of Karachi, Karachi, Pakistan.

Abstract

Lornoxicam is a Biopharmaceutics Classification System (BCS) Class II drug prescribed for rheumatoid arthritis and osteoarthritis. It is potent analgesic and anti-inflammatory agent but has poor aqueous solubility (pka 4.7) that reduces its oral absorption and pharmacological effect. The aim of the present study was to formulate polymeric nanoparticles of lornoxicam with increase aqueous solubility and better anti-inflammatory effect using anti-solvent precipitation method. A 2^2 full factorial design was used taking chitosan and soluplus® as independent variables whereas average particle size (z-average), % drug release and polydispersity index (PDI) as dependent variables. Four formulations fabricated, subjected to dynamic light scattering, *in-vitro* drug release (pH 1.2 HCl and pH 6.8 phosphate buffer), PDI and encapsulation efficiency. The results showed good characteristic features of trial formulations in nanodimensions. The formulation (F1) containing chitosan (80mg) and soluplus® (4mg) was selected as an optimized formulation due to less z -average (198.7±2.95nm) and PDI (0.225±0.01), stable zeta potential (-16.87±1.95) and maximum % drug release in pH 6.8 phosphate buffer (89.14±0.67%; $p<0.05$) comparatively to pure lornoxicam. The optimized formulation followed first order kinetics based on high R^2 (0.98), low AIC (48.79) and high MSC (3.64). The drug release mechanism was studied by Higuchi model that showed diffusion and erosion pattern with good correlation coefficient. Atomic force microscopy, Fourier transform Infrared, Thermogravimetric differential scanning calorimetry and X-ray powder diffraction characterization of the optimized formulation revealed its spherical shape, stable and semi crystalline structure and well polymeric encapsulation. The F1 formulation exhibited dose dependent results at 0.1mg/kg (56.55%;$p< 0.005$) and

Xi'an Shiyou Daxue Xuebao (Ziran Kexue Ban)/
Journal of Xi'an Shiyou University, Natural Sciences Edition
ISSN: 1673-064X
E-Publication: Online Open Access
Vol: 67 Issue 04 | 2024
DOI: 10.5281/zenodo.11063869

0.3mg/kg (81.11%;p<0.005) with IC_{50} 0.06mg/kg comparatively to pure lornoxicam for the same and higher doses (1mg/kg) respectively (p<0.005). Thus, the chitosan and soluplus® in combination at higher levels appeared to be best combination in formulating lornoxicam nanoparticles that successfully enhanced aqueous solubility, % drug release and pharmacological effect. *In-vivo* human studies of lornoxicam nanoparticles, its role in arthritis model are recommended for future researches.

Keywords: Anti-inflammatory, Chitosan, Drug Release, Lornoxicam, Polymeric Nanoparticles, Solubility, Soluplus®.

1. INTRODUCTION

Polymeric Nanotechnology based drug delivery systems are effectively used for the improvement of poor solubility and oral bioavailability of hydrophobic drugs. They not only provide ease of administration but also penetrates via epithelial and capillary membrane that allows efficient delivery of hydrophobic drugs (Sharma et al., 2019). In polymeric nanoparticles, drug particles are dispersed in aqueous medium (less than 1µm in diameter) and stabilized with the aid of stabilizer. The less particle size provides large surface area and aid in controlled delivery of drug for prolong period of time thereby reducing dose frequency. Various methods have been employed for preparation of nanoparticles such as ionic gelation method, anti-solvent precipitation method, high pressure homogenization etc. (Agarwal et al., 2018; Rahim et al., 2019; Ambrus et al., 2022). The polymeric nanotechnology is considered as an ideal platform for drugs having short half-life such as lornoxicam (Yarraguntla et al., 2016).

Lornoxicam, congener of tenoxicam is relatively a new non-steroidal anti-inflammatory drug (NSAID) belongs to oxicam class (Figure 1). It is Biopharmaceutics Classification System (BCS) class II drug possessing low solubility and high permeability available in the market in oral and parenteral dosage forms. It has excellent analgesic, anti-pyretic and anti-inflammatory properties in postoperative pain, inflammation and rheumatoid arthritis (Vengala and Vanamala, 2018). Due to its strong inhibition of prostaglandin biosynthesis, it differs from other NSAIDs and supposed similar to opioid analgesic (Helmy et al., 2017). But the extreme hydrophobic nature of lornoxicam limits its use in medicine despite of being potent anti-inflammatory drug which emerges the need of rectifying its hydrophobicity.

In a previous study, Vengala and Vanamala, (2018) increased lornoxicam dissolution rate using PVP K30 and β- cyclodextrin via antisolvent precipitation method. Helmy et al. (2017) formulated lornoxicam loaded nanomiceles using tetronic® and synperonic® polymers for intraperitoneal administration. Yarraguntla et al. (2016) formulated lornoxicam using polyvinyl pyrrolidone (PVP) and β- cyclodextrin while Sunita and Avinash, (2014) fabricated lornoxicam nanosuspension using poloxamer 407. The literature search clearly revealed lack of data in terms of oral lornoxicam nanoparticle formulations and only few synthetic excipients has been tried for enhancing its solubility.

Xi'an Shiyou Daxue Xuebao (Ziran Kexue Ban)/
Journal of Xi'an Shiyou University, Natural Sciences Edition
ISSN: 1673-064X
E-Publication: Online Open Access
Vol: 67 Issue 04 | 2024
DOI: 10.5281/zenodo.11063869

Chitosan is natural occurring biocompatible and biodegradable hydrophilic biopolymer extensively studied in improvisation of the solubility of poor soluble drugs, delivery of anti-cancer drug, genes, antigens, and therapeutic proteins etc. (Figure 1) (Sharma et al., 2019). It is cationic polysaccharide obtained from crustacean shells and fungal cell walls composed of randomly dispersed β-1-4 linked D-glucosamine and N-acetylglucosamine (Yegireddy et al., 2022). It is non-toxic, non-immunogenic and bio-adhesive in nature (Sharma et al., 2019). Therefore, US FDA has approved chitosan for nanoparticle drug delivery system. Literature indicates that chitosan possessing nanoparticles exhibits solubility enhancement, more drug absorption by protecting gastrointestinal lumina, controlled drug release, permeability enhancement and efflux inhibition (Yegireddy et al., 2022).

Soluplus® (polyvinyl caprolactam–polyvinyl acetate–polyethylene glycol graft copolymer) is relatively a new polymer which is amphipathic in nature synthesized primarily for solid solutions (Figure 1). Due to its amphiphilic nature it behaves as suitable stabilizer in nanoparticles by inhibiting agglomeration and Ostwald ripening phenomenon. Soluplus® reduces the interfacial tension of particle surface via an attractive water surfactant interaction thereby stabilizes fine particles (Yang et al., 2014).

Therefore, the aim of current study was to increase the aqueous solubility, providing controlled drug release and effective *in-vivo* anti-inflammatory activity of lornoxicam in oral nanoparticles utilizing chitosan and soluplus® in combination through anti-solvent precipitation method.

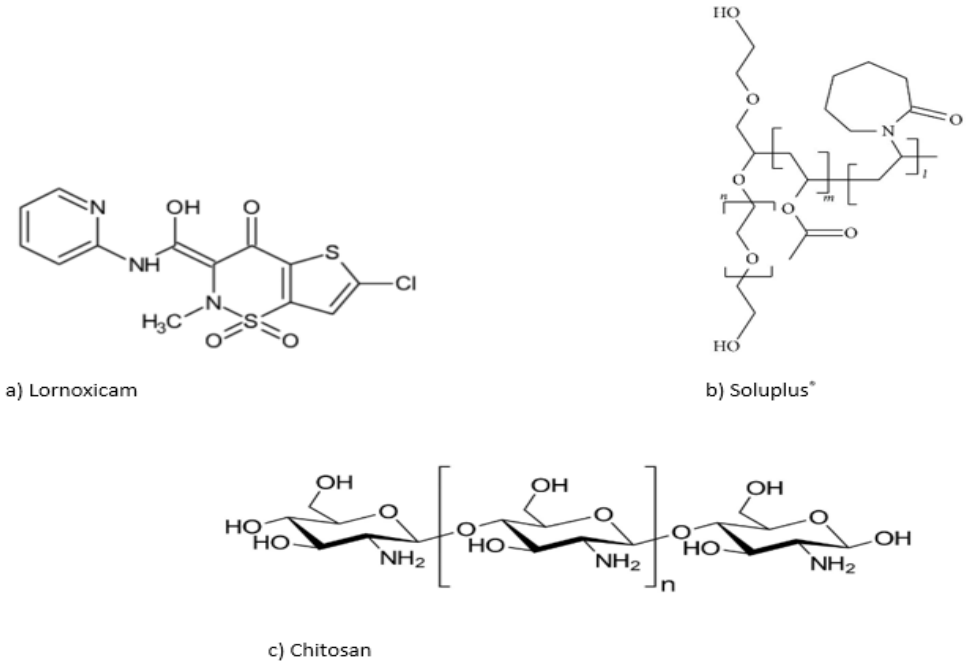

Figure 1: Chemical Structures of a) Lornoxicam b) Soluplus® c) Chitosan

Xi'an Shiyou Daxue Xuebao (Ziran Kexue Ban)/
Journal of Xi'an Shiyou University, Natural Sciences Edition
ISSN: 1673-064X
E-Publication: Online Open Access
Vol: 67 Issue 04 | 2024
DOI: 10.5281/zenodo.11063869

2. MATERIALS AND METHODS

Lornoxicam was kindly gifted by Getz Pharma (Pvt.) Ltd. Pakistan and Soluplus® (MW: 90000-140000g/mol) was obtained from BASF, Germany. Carrageenan and Chitosan (≤75% deacetylated) were obtained from Sigma Aldrich. Dimethyl sulfoxide (DMSO) was bought from BioM Laboratories, Cerritos, USA. Glacial acetic acid, Sodium Hydroxide and Potassium dihydrogen phosphate were purchased from Merck Germany.

2.1. Animals

Male and female albino Wistar rats (180-200 g) were bought from H.E.J. Research Institute of Chemistry, University of Karachi. All experiments were performed in the Department of Pharmacology, Faculty of Pharmacy & Pharmaceutical Sciences, University of Karachi. Ethical guidelines given by Association for Assessment and Accreditation of laboratory Animal Care International (AAALAC) were followed throughout the study. Institutional Bioethical Committee, University of Karachi gave clearance (IBC KU-316/2023) to use experimental animals for the study. Animals fed standard diet and water and kept under regulated temperature (22 ± 2 °C), relative humidity (50 ± 10%) and 12 hours' light and dark cycle.

2.2. Methods

In this study, 2^2 full factorial design was employed with two factors at two levels (low and high) to determine the effect of factors, variables and their combined effect at both levels on average particle size (z-average), polydispersity index (PDI) and *in-vitro* % drug release. Chitosan and soluplus® were used as independent variables whereas z-average, PDI, *in-vitro* % drug release was taken as dependent variables (Table 1). A total of four formulations were fabricated out of which one selected as optimized formulation on the basis of least z-average, low PDI, and maximum % drug release. The optimized nanoparticle led to various characterization parameters including atomic force microscopy (AFM), Fourier transform infrared (FTIR) spectroscopy, Thermogravimetric differential scanning calorimetry (TGA-DSC) and X-ray diffraction (XRD) to determine surface morphology, drug polymer interaction, stability and purity and crystallinity respectively. Following characterization studies the optimized formulation was subjected to anti-inflammatory activity in rats to ascertain pharmacological effects in comparison to pure lornoxicam.

2.3. Preparation of Lornoxicam nanoparticles

Lornoxicam nanoparticles were formulated using anti-solvent precipitation method. In this method 20 mg lornoxicam was accurately weighed and dissolved in DMSO (solvent). It was added dropwise into aqueous medium containing appropriate proportions of 1% chitosan and soluplus® (anti-solvent) (Table 1) with continuous stirring at 8000 rpm under cold condition. The mixture was kept stirring to become milky suspension, sonicated well for 15 minutes and left overnight in refrigerator (Shariare et al., 2019; Vengala and Vanamala, 2018).

Xi'an Shiyou Daxue Xuebao (Ziran Kexue Ban)/
Journal of Xi'an Shiyou University, Natural Sciences Edition
ISSN: 1673-064X
E-Publication: Online Open Access
Vol: 67 Issue 04 | 2024
DOI: 10.5281/zenodo.11063869

The milky nanoparticles were centrifuged at 13000 rpm for 25 minutes at 4°C. The supernatant was collected into glass vials for the evaluation of EE % and the sediment nanoparticles were freeze dried at -70°C for 24 hour using Operon freeze dryer, FDB-7003, Korea. The freeze-dried nanoparticles stored in refrigerator for further characterization studies.

Table 1: A 2^2 full factorial design showing Lornoxicam nanoparticles formulations

Formulation Codes	Amount of lornoxicam (mg)	Independent variables			
		Chitosan (Coded value)	Soluplus® (Coded value)	Chitosan (mg)	Soluplus® (mg)
F1	20	(+)	(+)	80	4
F2	20	(-)	(-)	40	2
F3	20	(+)	(-)	80	2
F4	20	(-)	(+)	40	4

Fn = Formulation with respective number, (+) corresponds to high level, (-) corresponds to low level

3. CHARACTERIZATION OF NANOPARTICLES

3.1. Z-average, PDI and zeta potential

Z-average, PDI and zeta potential values of all formulations of lornoxicam nanoparticles were estimated using dynamic light scattering technique (DLS) by Malvern Zetasizer ZS (Malvern Instrument, Worcestershire, United Kingdom). Each sample was prepared in distilled water as 10 µl/ml, sonicated well for 10min to convert into proper homogenous mixture for DLS study (Khan et al., 2022). Samples ran in triplicate to obtain mean±SD of each formulation.

3.2. AFM

The surface morphology of nanosized particles from optimized formulation was determined using AFM (5500, ACAFM, Agilent Technologies). The optimized nanoparticles were dispersed in distilled water. The equipment operated in tapping mode and equipped with a silicon nitride probe, the sample scanned using Mica sheet sample substrate at resonance frequency of 298.563 kHz. The data was analyzed via Pico View 1.12.2 software (Aslam et al., 2020).

3.3. FTIR

The IR spectra of pure lornoxicam, chitosan, soluplus® and optimized nanoparticles were scanned under FTIR spectrophotometer (IR-Prestige-21, Shimadzu) using potassium bromide (KBr) disc method. Sample was mixed with KBr in 1:40 ratio and converted into disc via applied pressure and placed into chamber. FTIR spectra were obtained in the range of 4000 to 400 cm^{-1} wave number. IR solution software was used to analyze data (Naik et al., 2021).

Xi'an Shiyou Daxue Xuebao (Ziran Kexue Ban)/
Journal of Xi'an Shiyou University, Natural Sciences Edition
ISSN: 1673-064X
E-Publication: Online Open Access
Vol: 67 Issue 04 | 2024
DOI: 10.5281/zenodo.11063869

3.4. TGA-DSC

The stability and purity of pure lornoxicam and freeze-dried optimized nanoparticles was determined using TGA-DSC (DSC SDT 650, TA Instruments, and New Castle, DE, USA). Around 5 mg sample was kept in sample holder, taken aluminium empty reference holder as standard and analyzed from 25-500°C with 15°C/min rate. Nitrogen was continued at 99.98ml/min flow rate. TRIOS Software was used to analyze the data (Shariare et al., 2019).

3.5. XRD

The XRD patterns for pure lornoxicam and optimized nanoparticles were determined under PANalytical X-pert Pro X-ray diffractometer (DY3313, Amsterdam, and The Netherlands). Nitrogen filtered CuK-alpha radiation (wavelength 1.5418 A) was used as source of X-ray. The X-ray tube ran at a power of 40 kV, 30 mA. Approximately 60 mg sample was scanned from 10 to 80° 2θ with 0.6s step time and 0.0250° step size (Modi and Tayade, 2006).

3.6. EE%

EE % was calculated by measuring absorbance of supernatant collected after centrifugation of samples at 13000 rpm for 25 min. at 4°C temperature using cool ultracentrifuge (Jouan, MR 22i Refrigerated Centrifuge, France). The absorbance was taken at λ=376nm using UV visible spectrophotometer (UV-1800, Shimadzu) against distilled water as blank. Samples ran in triplicate and measurements were taken as mean±SD of each sample (Subbiah et al., 2021).

The EE % was calculated using following formula;

$$\text{EE } (\%) = \frac{\text{Amount of drug loaded into nanoparticles}}{\text{Amount of drug used for nanoparticles}} \times 100$$

3.7. Drug Release study (%)

The drug release study of all formulations of lornoxicam nanoparticles was carried out in dialysis membrane using dialysis bag diffusion technique. Freeze dried samples equivalent to 4 mg lornoxicam was transferred to dialysis membrane after making dispersion in distilled water, tied accurately and placed into USP dissolution apparatus (USP Type II – paddle type) containing 900 ml phosphate buffer (pH 6.8). The apparatus was set at 37°±0.5°C and operated at 50 rpm.

The samples were withdrawn at 5, 15, 30, 60, 120, 180, 240, 300 min. and replaced with the equal volume of fresh dissolution medium maintained at the same temperature. The absorbance of collected samples was noted at λ_{max} of drug (Yarraguntla et al., 2016). The same procedure followed for pH 1.2 (0.1 N HCl).

Xi'an Shiyou Daxue Xuebao (Ziran Kexue Ban)/
Journal of Xi'an Shiyou University, Natural Sciences Edition
ISSN: 1673-064X
E-Publication: Online Open Access
Vol: 67 Issue 04 | 2024
DOI: 10.5281/zenodo.11063869

3.8. *In-vitro* Drug Release Kinetics

The drug release data of optimized nanoparticles in both media were subjected to various kinetic models to determine the best fit model. The model selection criteria were based on high correlation coefficient (R^2), low Akaike information criterion (AIC) and high model selection criterion (MSC). The model studied included zero order, first order, Higuchi, Hixon Crowell, Korsemeyer-Peppas and Weibull.

3.9. Experiments in animals

3.9.1. *In-vivo* cytotoxic study

In-vivo cytotoxic study was carried out using standard MTT (3- [4, 5-dimethylthiazole-2-yl]-2, 5-diphenyl-tetrazolium bromide) colorimetric assay in which mouse fibroblast (3T3 cell line) was used as indicated in literature (Mosmann, 1983). 3T3 (mouse fibroblast) cells were cultured in 75 cm^2 flasks containing Dulbecco's Modified Eagle Medium, supplemented with 5% of fetal bovine serum (FBS) and antibiotics (penicillin and streptomycin, 100 IU/ml each). It was kept in 5% CO_2 incubator at 37^oC. Exponentially growing cells were harvested, counted with haemocytometer and diluted with a particular medium. Cell culture was prepared in 5x10^4cells/ml concentration and filled 100 µL/well into 96 well plates.

The culture media was changed with 200 µL of fresh medium containing various concentrations of reference standard (doxorubicin) and optimized formulation F1 (1-30µM) after overnight incubation. Then, each well was filled with MTT (200 µL; 0.5mg/ml) after 48 hours and incubated for another 4 hours. Later, each well filled with 100 µL, DMSO. MTT was reduced to formazan within cell and its extent was determined by taking absorbance at 540nm using microplate reader (Spectra Max plus, Molecular Devices, CA, USA). The cytotoxicity was recorded as concentration causing 50% growth inhibition (IC_{50}) for 3T3 cells. Formula used for % inhibition is as under:

$$\% \text{ Inhibition} = 100 - \frac{((\text{Mean of O.D.of test compound} - \text{Mean of O.D.of negative control})}{\text{Mean of O.D.of positive control} - \text{Mean of O.D.of negative control})} \times 100)$$

Where; O.D. = Optical density

3.9.2. Anti-inflammatory activity

The anti-inflammatory test of pure lornoxicam and optimized nanoparticles, F1 was performed in albino Wistar rats of both sexes (180 to 220g). The animals were distributed equally in three groups. Each group contained n=3 animals per dose. Group 1 taken as control (Vehicle control=10% DMSO). Group 2 and group 3 were given pure lornoxicam and F1 respectively in doses 0.01, 0.1 and 1mg/kg with the difference of 0.3mg/kg in F1 instead of 1mg/kg. The volume of dose was 5ml/kg. After half hour (h) of oral dose subplantar injection of 0.1 ml 1% carrageenan injection was administered into right hind paw of each rat. The experiment repeated thrice to obtain total n=9 animals for each dose in a group.

Xi'an Shiyou Daxue Xuebao (Ziran Kexue Ban)/
Journal of Xi'an Shiyou University, Natural Sciences Edition
ISSN: 1673-064X
E-Publication: Online Open Access
Vol: 67 Issue 04 | 2024
DOI: 10.5281/zenodo.11063869

The paw thickness was measured using digital Vernier calipers just before injection and each after 0.5, 1, 2 up to 5 h. The % inhibition of inflammation was determined using formula;

$$\text{Inhibition of inflammation } (\%) = 1 - \frac{(\text{Ct} - \text{C0})\ \text{treated group}}{(\text{Ct} - \text{C0})\ \text{control group}} \times 100$$

Where;

C0 is mean paw thickness measured at time 0 h and Ct is the mean paw thickness measured at particular time point (Engelhardt et al., 1995; Li et al., 2020).

3.10 Statistical evaluation

The data is displayed as Mean ± Standard Deviation (SD) for physicochemical tests. Drug release data was evaluated using One Way Analysis of Variance (ANOVA) using $p<0.05$ as significant value. The drug release *in-vitro* kinetics models such as Zero order, first order, Higuchi, Hixson-Crowell, Korsemeyer-Peppas and Weibull were applied using DD solver^R software to get the best fit model.

Anti-inflammatory data is displayed as Mean ± Standard error of mean (SEM) of n= 3 independent experiments. IC_{50} (mg/kg) was calculated graphically using linear regression analysis via MS Excel 2019 (n=3). Anti-inflammatory results were analyzed using one-way ANOVA followed by post hoc least significant difference (LSD) and Duncan tests. The Software SPSS version 20 was used to analyze the data with $p<0.05$ as significant value. LSD was used to compare control and treatment groups while Duncan analyzes intergroup differences.

4. RESULTS AND DISCUSSION

The objectives of present work were to formulate polymeric nanoparticles of lornoxicam using chitosan and soluplus® with increase aqueous solubility, % drug release and improved anti-inflammatory effect by antisolvent precipitation method. The resulting trial formulations were subjected to physicochemical tests and characterization using various techniques followed by *in-vivo* pharmacological activity in rats' model.

4.1. Z-average, PDI, zeta potential and EE%

All four formulations of lornoxicam nanoparticles were subjected to DLS technique and resulted in z-average ranged from 198.7±2.95 to 568.0±4.03nm, PDI 0.22±0.01 to 0.75±0.09 and zeta potential -9.35±0.84 to -16.87±1.95 (Table 2). Formulation, F1 contained high levels of both chitosan (80mg) and soluplus® (4mg) (Table 1) contributed in reducing the particle size more than other formulations. The high level of chitosan produced optimum concentration required for reduced particle size consistent with previous findings by creating more cross linkages between drug and chitosan (Mirtajaddini et al., 2021) which was enhanced at high level of soluplus® in the present study. Soluplus® due to its strong amphiphilic property made good surface activity thereby reducing interfacial tension between drug molecule and water by allowing more water

Xi'an Shiyou Daxue Xuebao (Ziran Kexue Ban)/
Journal of Xi'an Shiyou University, Natural Sciences Edition
ISSN: 1673-064X
E-Publication: Online Open Access
Vol: 67 Issue 04 | 2024
DOI: 10.5281/zenodo.11063869

surfactant interaction hence produced small particle size. All formulations showed adequate stability indicating zeta potential values. But F1 with -16.87±1.95 value indicated stronger nanoparticles ensuring good colloidal stability. From the results of PDI it is evident that F1 and F3 exhibited homogenous and fairly narrow particle size distribution due to less than 0.3 PDI while F2 and F4 formed heterogenous dispersions owed to high PDI (more than 0.3). The results found in agreement with previous findings (Yegireddy et al., 2022; Sutradhar et al., 2013; Salarbashi et al., 2021).

The EE % of all nanoparticle formulations ranged from 74.48±0.28% to 88.87±0.33%. F1 indicated lowest EE % in all formulations due to the presence of more gelling property of chitosan in higher concentration which hinders the EE% (Sharma et al., 2019). The effect of high level of soluplus® might suppressed in F1 due to more gelatinous property of chitosan causing less drug to be encapsulated in the nanoparticles compared to other formulations. Chitosan at low level (40mg) in F2 encapsulated more drug at low (2mg) level of soluplus® but when its level became high in F3 with low level of soluplus® showed more encapsulation of drug (Table 2). Soluplus® in high concentration encapsulate more drug as indicated by Jin et al. (2020) but in the present study its role might be suppressed due to gelatinous nature of chitosan. From these results F1 seems optimized formulation because of least z-average, PDI and stabilized zeta potential (Figure 2).

Table 2: Physicochemical characteristic features of lornoxicam nanoparticles formulations

Formulation Codes	EE±SD (%)	Z-average ±SD (nm)	PDI±SD	Zeta potential ±SD	%Drug Release±SD (pH 6.8 phosphate buffer; 5h)	%Drug Release±SD (pH 1.2 HCl; 5h)
F1	74.48±0.28	198.7±2.95	0.225±0.01	-16.87±1.95	89.14±0.67	52.63±1.15
F2	86.63±0.42	568.0±4.04	0.757±0.09	-9.35±0.84	67.05±0.89	24.97±1.37
F3	88.87±0.33	262.5±5.25	0.284±0.07	-11.53±1.11	71.05±1.34	35.86±1.17
F4	79.58±0.58	217.7±2.49	0.696±0.02	-15.76±1.84	84.37±1.40	45.33±2.68

Where Fn=Formulation with respective numbers, EE=Encapsulation Efficiency, Z-average= average particle size, PDI= Polydispersity index, SD= Standard deviation

Xi'an Shiyou Daxue Xuebao (Ziran Kexue Ban)/
Journal of Xi'an Shiyou University, Natural Sciences Edition
ISSN: 1673-064X
E-Publication: Online Open Access
Vol: 67 Issue 04 | 2024
DOI: 10.5281/zenodo.11063869

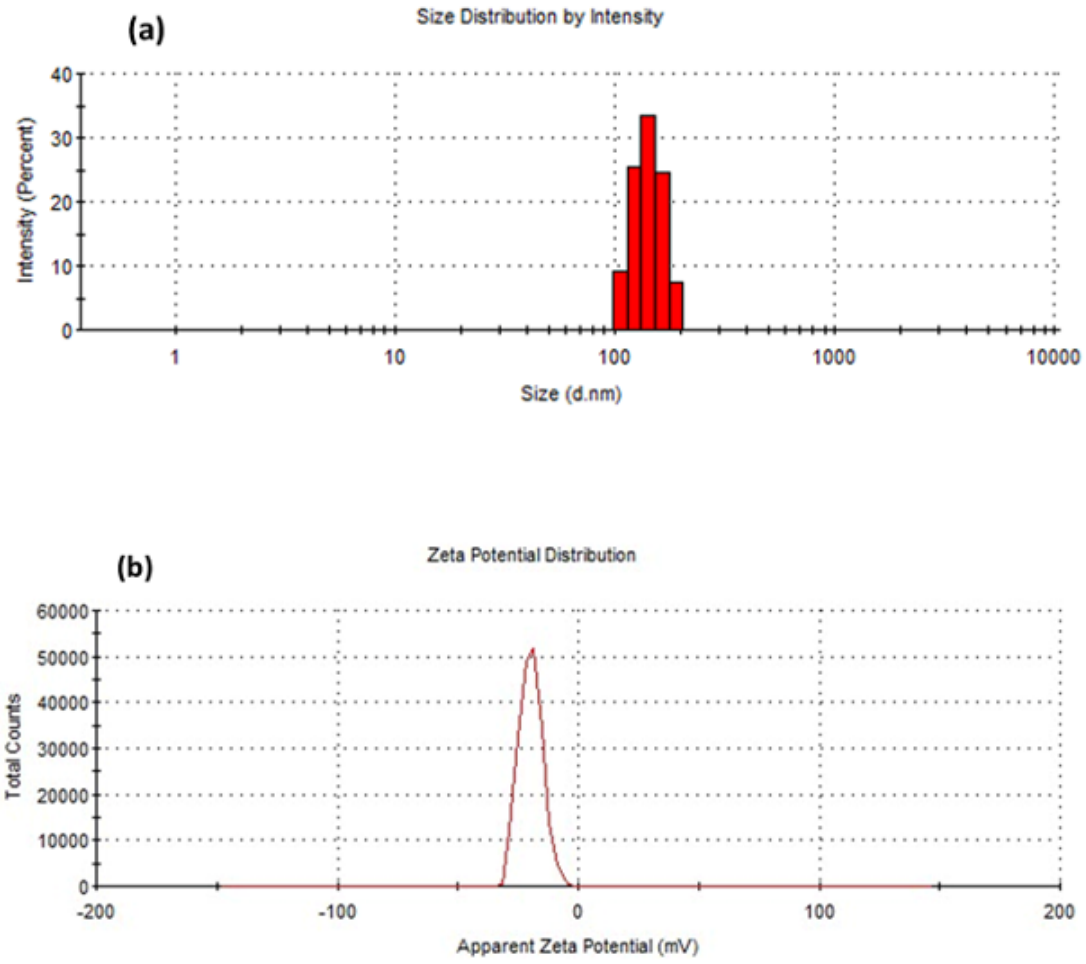

Figure 2: Z-average (a) and zeta potential (b) of F1 by DLS technique

4.2. AFM

AFM of nanoparticles is important to understand particle shape and surface morphology. The surface regularity and shape of particles influences surface area which ultimately improves solubility and drug release (Yarraguntla et al., 2019; Vengala and Vanamala, 2018). Therefore, AFM of optimized nanoparticles, F1 was analyzed. The morphology of F1 displayed somewhat spherical particles having smooth surface. The maximum particle size was 28.1nm. The histogram showed size range from 14 to 28.1nm (Figure 3). The topography of 2D and 3D images indicated smooth, uniform, mostly non-aggregated and well distributed particles supporting PDI findings (Table 2).

Xi'an Shiyou Daxue Xuebao (Ziran Kexue Ban)/
Journal of Xi'an Shiyou University, Natural Sciences Edition
ISSN: 1673-064X
E-Publication: Online Open Access
Vol: 67 Issue 04 | 2024
DOI: 10.5281/zenodo.11063869

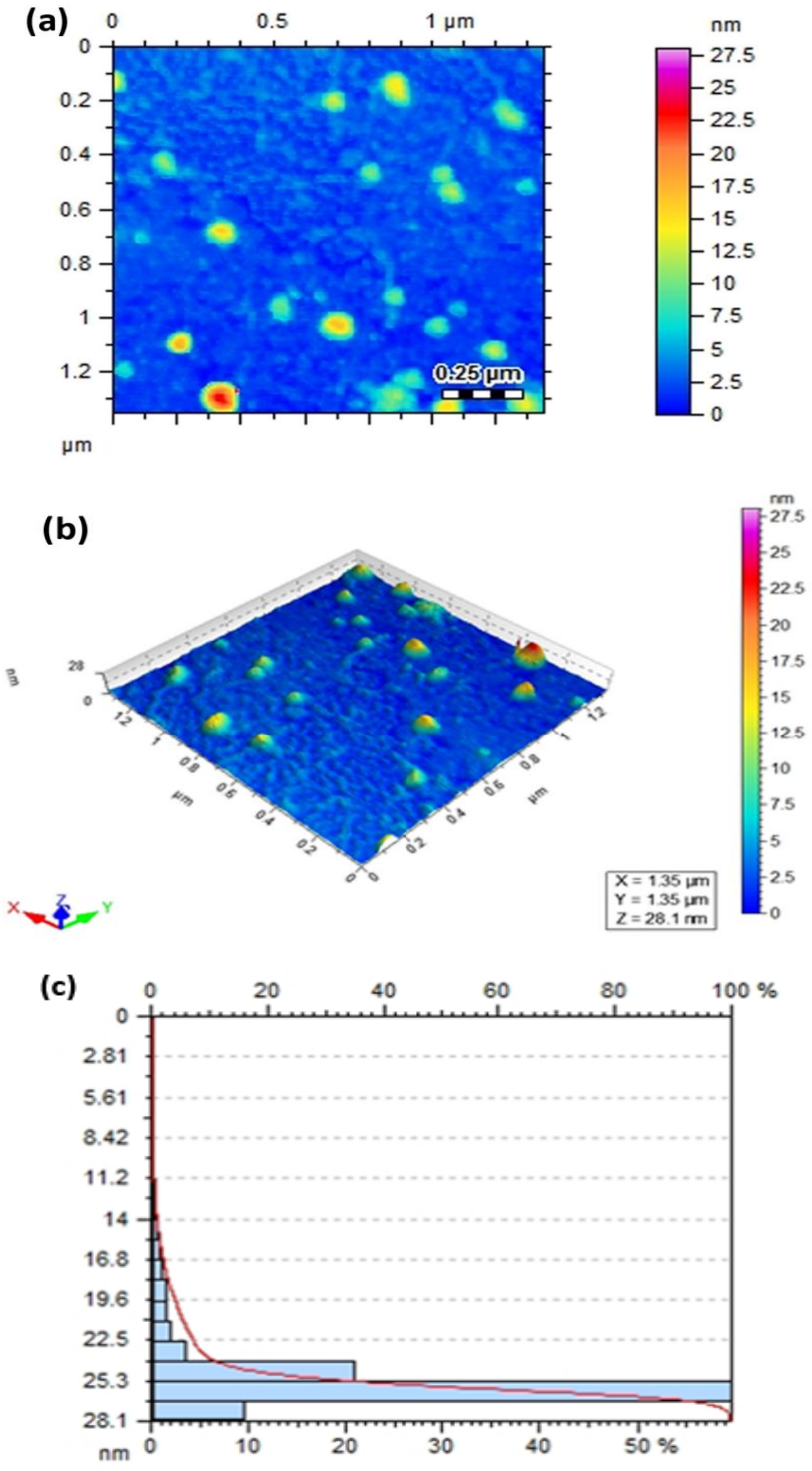

Figure 3: AFM images of F1 (a) 2D image (b) 3D image (c) histogram

Xi'an Shiyou Daxue Xuebao (Ziran Kexue Ban)/
Journal of Xi'an Shiyou University, Natural Sciences Edition
ISSN: 1673-064X
E-Publication: Online Open Access
Vol: 67 Issue 04 | 2024
DOI: 10.5281/zenodo.11063869

4.3. FTIR

FTIR overlay spectra of pure lornoxicam, chitosan, soluplus® and F1 are shown in Figure 4. In the spectrum of pure lornoxicam characteristic peaks at 3066.82 cm^{-1}, 1635.64cm^{-1} and 1597.06 cm^{-1} represented NH group stretching vibration, stretching vibration in C=O group of primary amide and NH group bending vibration in secondary amide respectively. Peaks at 1386.82 cm^{-1} and 1330.88 cm^{-1} were assigned to stretching vibrations of SO_2 group while peak at 783.1 cm^{-1} represented C-Cl bending (Almotairi et al., 2022, Sunita and Avinash, 2014).

FTIR spectrum of chitosan indicated a broad band at 3448.72 cm^{-1} corresponding to NH and OH stretch collectively (Hassani et al., 2014) due to strong intermolecular hydrogen bonding. Amide I and amide II peaks appeared at 1653.00 cm^{-1} (C=O stretching in amide group) and 1591.27 cm^{-1} (NH bending in amide group) respectively (Li et al., 2011, Agarwal et al., 2018). The C-CH3 bending vibration appeared at 1386.82 cm^{-1} (Subbiah et al., 2021).

FTIR spectrum of soluplus® revealed distinguishing peaks of OH stretch alcohol and C-H stretching at 3442.94 cm^{-1} and 2926.01 cm^{-1} respectively (França et al., 2018). The regions of carbonyl (CO) bands found in soluplus® in between 1800 cm^{-1} and 1400cm^{-1}. The strong absorption bands in soluplus® reflects the carbonyl stretching vibrations of the caprolactam ring. The CO frequencies of soluplus® at 1624.06 cm^{-1} and 1741.72cm^{-1} were related to amide and ester groups respectively (Lan et al., 2010).

The optimized formulation, F1 showed all peaks of lornoxicam and chitosan with low intensity and slight shift in wavenumber ensuring drug encapsulation in polymer. A less intense peak of NH group stretching vibration of lornoxicam appeared at 3070.68 cm^{-1} in F1. This indicated partial interaction of soluplus® with lornoxicam. The stabilizer soluplus® appeared in F1 with shift in wavenumber.

The peaks at 1741 cm^{-1} ($OCOCH_3$ or ester group) and 1624 cm^{-1} (amide group) in soluplus® got disappeared from F1 indicating drug encapsulation in stabilizer.

The disappearance of peak and shift in wavenumber in F1 resulted in the interaction of amine and alcohol groups of lornoxicam with carbonyl group of soluplus® through hydrogen bonding and less intense peaks appeared due to dilution effect of polymers in F1. These changes helped in significant formation of nanoparticles with no effect on drug stability as evident from TGA-DSC studies (Sunita and Avinash, 2014).

Xi'an Shiyou Daxue Xuebao (Ziran Kexue Ban)/
Journal of Xi'an Shiyou University, Natural Sciences Edition
ISSN: 1673-064X
E-Publication: Online Open Access
Vol: 67 Issue 04 | 2024
DOI: 10.5281/zenodo.11063869

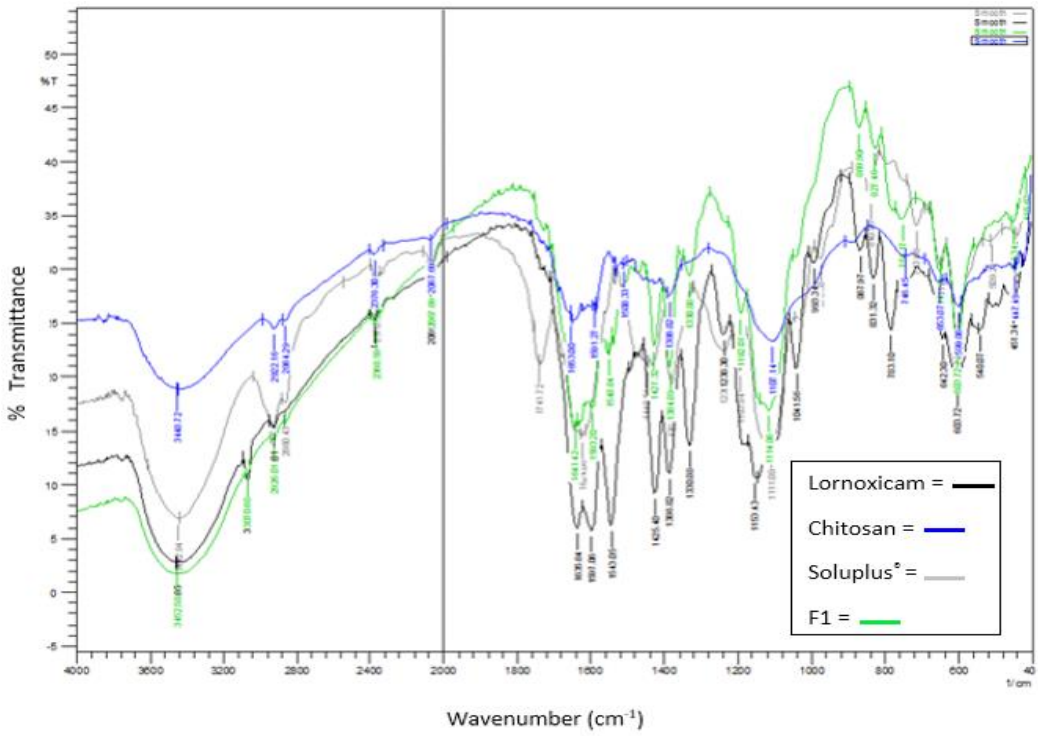

Figure 4: FTIR overlay spectra of lornoxicam, Chitosan, Soluplus® and F1

4.4. TGA-DSC

The purity, stability and thermal degradation of pure lornoxicam and F1 was determined by TGA-DSC study. The DSC curve of pure lornoxicam showed endothermic peak at 216.22°C which was closed to its melting point reported in literature indicated the crystallinity of drug (Almotairi et al., 2022). The combine TGA-DSC curves of pure lornoxicam and F1 are displayed in Figures 5 and 6 respectively. DSC curve of F1 showed endothermic peak at 241.46°C, corresponding to the increase in thermal stability of compound. The DSC thermogram of F1 indicated reduction in crystallinity of nanoparticles due to change in peak intensity that might contributed its enhanced solubility, drug release and therapeutic effect.

TGA curve of pure lornoxicam showed initial degradation at 206°C with almost complete degradation over 300°C (Figure 5). TGA curve of F1 showed a slow pattern of degradation process as seen from Figure 6. The initial degradation occurred at 160.66°C probably due to moisture loss present in the compound. Then second event of thermal degradation around 250° to 300°C indicated the decomposition of chitosan and soluplus® in the nanoparticles (Twal et al., 2024). Therefore, from TGA-DSC curve it was noticed that crystallinity of drug reduced in F1 owing to change in thermogram and drug related stability of nanoparticles increased due to encapsulation of drug into chitosan and soluplus® as evident from high melting point in F1 and gradual degradation pattern from TGA-DSC curve (Güncüm et al., 2018, Carvalho et al., 2019).

Xi'an Shiyou Daxue Xuebao (Ziran Kexue Ban)/
Journal of Xi'an Shiyou University, Natural Sciences Edition
ISSN: 1673-064X
E-Publication: Online Open Access
Vol: 67 Issue 04 | 2024
DOI: 10.5281/zenodo.11063869

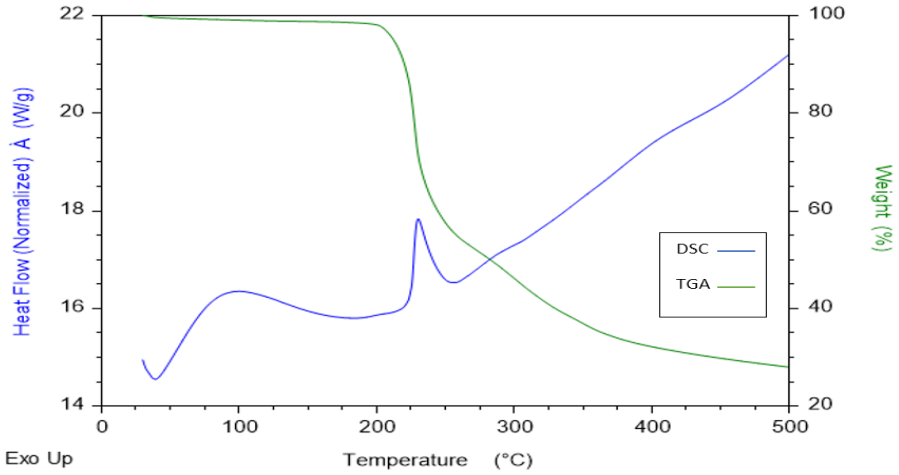

Figure 5: TGA-DSC curve of pure lornoxicam

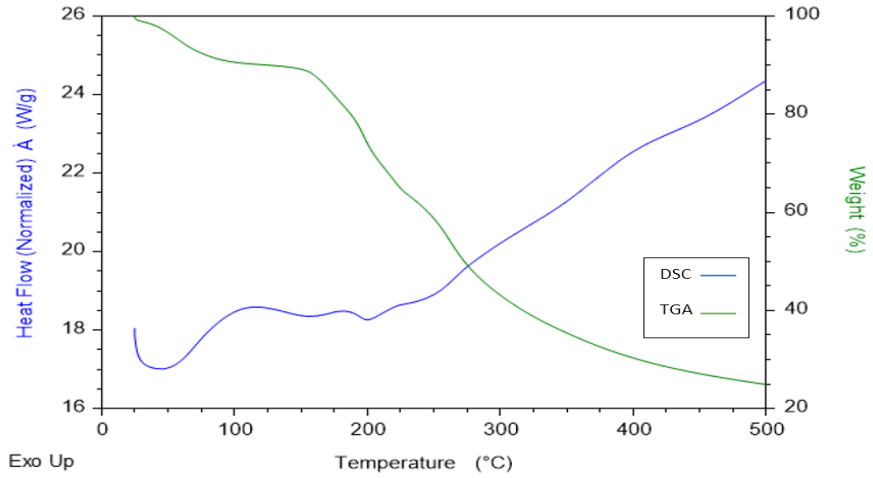

Figure 6: TGA-DSC curve of F1

4.5. XRD

XRD analysis is used to determine crystallinity of nanoparticles as compare to pure drug. The XRD patterns for pure lornoxicam and F1 are shown in Figure 7 which confirmed DSC (Figures 5 and 6) and FTIR (Figure 4). It can be revealed from Figure 7 that pure lornoxicam is crystalline in nature exhibiting sharp peaks at 2 θ values of 18.8°, 21.58°, 23.06°, 24.78°, 28.18°, 30.53°, 38.66° and 44.96°. F1 showed halo pattern while some sharp peaks are displayed at 2θ values of 38.56°, 44.76° and 72.71°. It indicated change in crystalline state of drug in nanoparticles and considered to be semi-crystalline in structure. This was due to particle size reduction from micron to nanosize that expected to aid in enhanced solubility and maximum controlled drug release (Sunita and Avinash, 2014). The semi-crystalline state might contribute in enhanced stability of drug supporting TGA-DSC studies (Figure 6).

Xi'an Shiyou Daxue Xuebao (Ziran Kexue Ban)/
Journal of Xi'an Shiyou University, Natural Sciences Edition
ISSN: 1673-064X
E-Publication: Online Open Access
Vol: 67 Issue 04 | 2024
DOI: 10.5281/zenodo.11063869

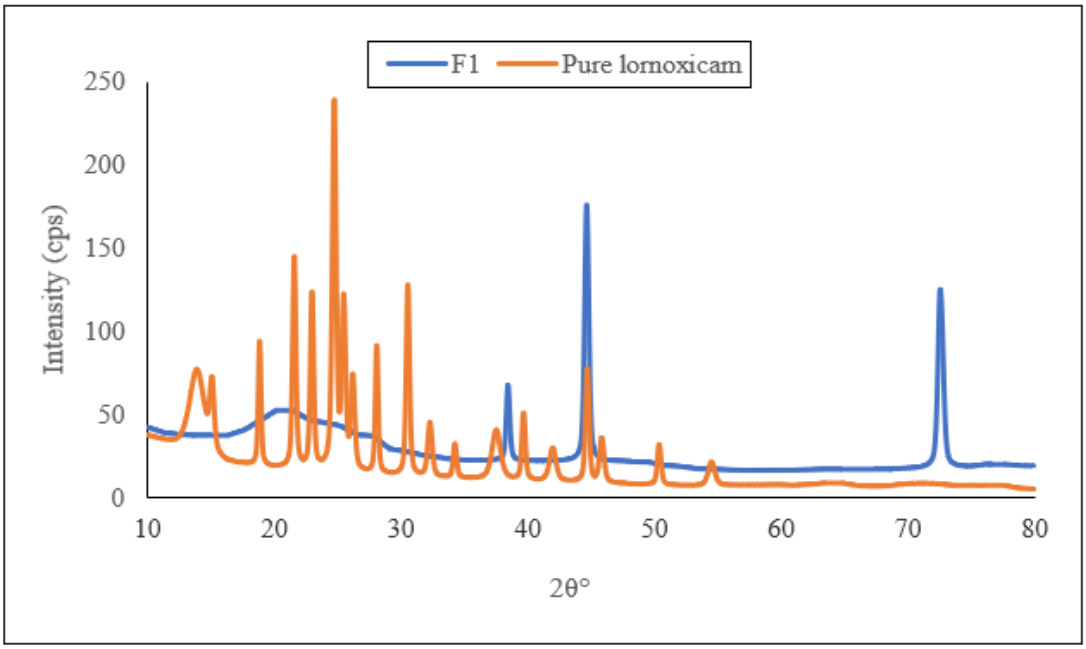

Figure 7: XRD overlay spectra of pure lornoxicam and F1

4.6. *In-vitro* Drug Release

The *in-vitro* drug release of all formulations of lornoxicam nanoparticles were determined in pH 1.2 (0.1 N HCl) and pH 6.8 phosphate buffer (Table 2; Figures 8 and 9). From the release profile it is evident that pure lornoxicam released slightly more in pH 6.8 phosphate buffer (25.95±1.95%) than pH 1.2 HCl (18.69±0.97%) till 300min (5 hours).

The low release pattern suggested hydrophobicity in dissolution media. In pH 1.2 HCl (0.1 N HCl) the maximum drug release was noted in F1 which showed initial burst release (19.77±0.38%) in the first 5 min. then a gradual increase in profile was noted till 5 hours up to 52.63±1.15%; $p<0.05$ (Table 2 and Figure 8). The initial burst release was due to the presence of surface bound drug over nanoparticles (Yuan et al., 2013).

In pH 6.8 phosphate buffer F1 showed much higher release than pH 1.2 HCl and gradually increased to 89.14±0.67%; $p<0.05$ till 5 hours which shows its high solubility in alkaline medium as supported by previous studies (Yarraguntla et al., 2016).

The gradual release of drug indicated its well encapsulation into polymer matrix. In F2 initial burst release of 36.19±0.63% in 5 min. was obtained due to free drug present over the surface of nanoparticles but it attained only 67.05±0.89% till 5 hours. In F3 slow release was noted and attained 71.05±0.34 % drug release till end.

In F4 24.27±1.79% drug released in early 5 min then gradual rise in graph was noted up to 84.37±1.4% (Table 2 and Figure 9). The results can be represented in both dissolution media in the descending order as F1>F4>F3>F2.

Xi'an Shiyou Daxue Xuebao (Ziran Kexue Ban)/
Journal of Xi'an Shiyou University, Natural Sciences Edition
ISSN: 1673-064X
E-Publication: Online Open Access
Vol: 67 Issue 04 | 2024
DOI: 10.5281/zenodo.11063869

In both media optimized nanoparticle found to be F1 as it contained high levels of both chitosan and soluplus® that contributed in increasing the solubility and dissolution of lornoxicam in comparison to its pure form. Both polymer and stabilizer possess strong hydrophilic property and soluplus® being amphiphilic in nature solubilizes the lornoxicam in its hydrophobic core and increases its diffusion in hydrophilic environment which was enhanced due to presence of chitosan.

Although chitosan has inherent gelling property so when it was in higher concentration it might cause a slow and gradual release from the beginning as noticed in F1 and F3 that aided in achieving controlled release of drug over 5 hours along with their narrow particle size distribution. These results can be correlated with previous studies (Sharma et al., 2019; Yegireddy et al., 2022).

However, F1 obtained less EE% but it showed better particle size distribution, more stable zeta potential and maximum drug release hence it was selected as optimized formulation among all formulations of nanoparticles.

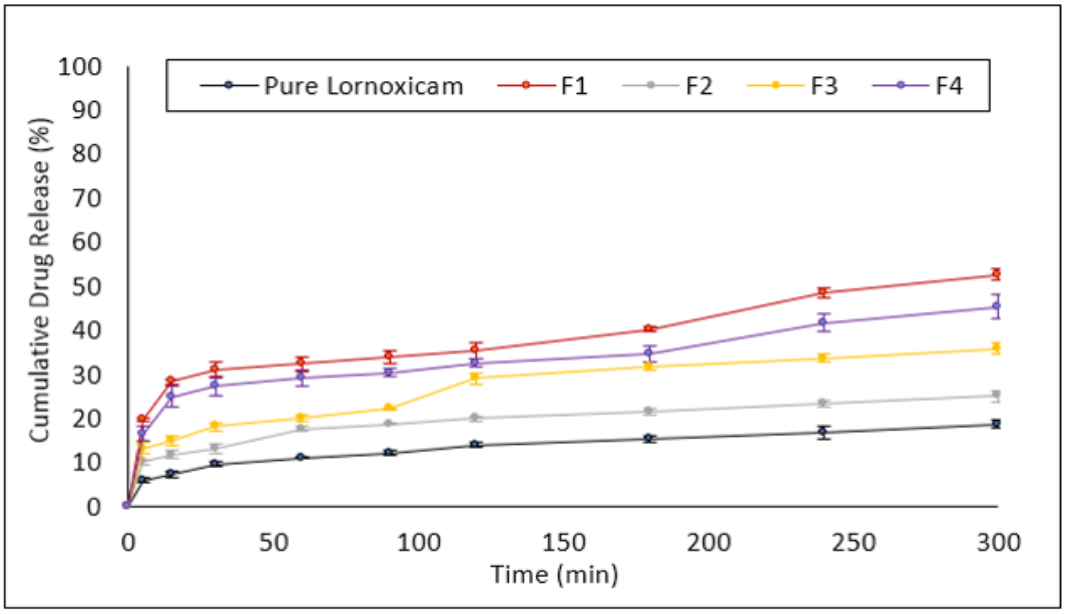

$p<0.05$

Figure 8: Lornoxicam cumulative % release profiles in HCl pH 1.2

Xi'an Shiyou Daxue Xuebao (Ziran Kexue Ban)/
Journal of Xi'an Shiyou University, Natural Sciences Edition
ISSN: 1673-064X
E-Publication: Online Open Access
Vol: 67 Issue 04 | 2024
DOI: 10.5281/zenodo.11063869

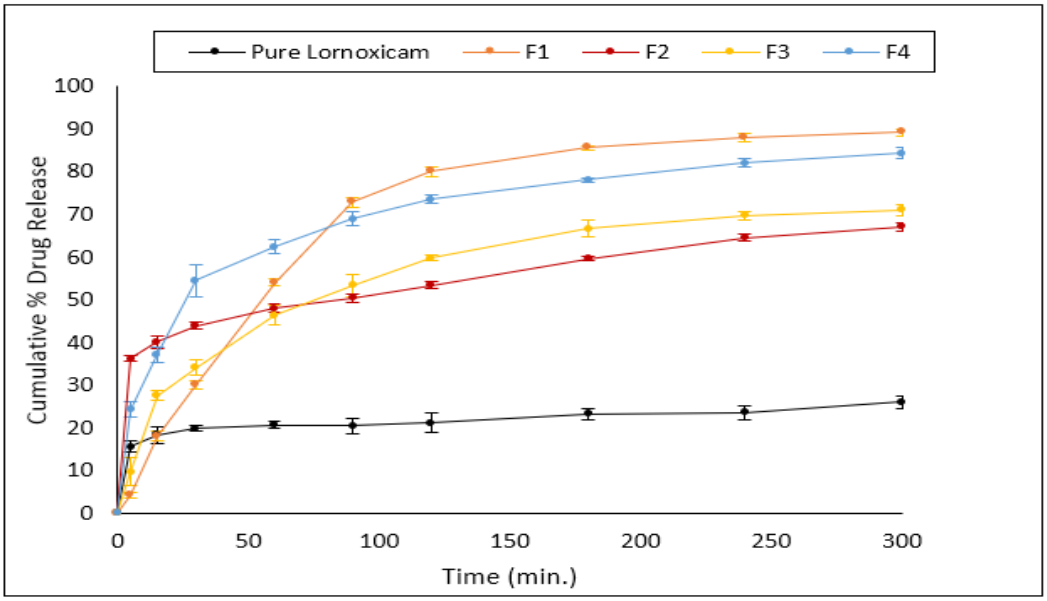

$p<0.05$

Figure 9: Lornoxicam cumulative % drug release profiles in phosphate buffer pH 6.8

4.7. *In-vitro* Drug Release Kinetics

Drug release data of optimized formulation, F1 was fitted into mathematical models to determine best fit model and mechanism of drug release in both media (pH 6.8 phosphate buffer and pH 1.2 HCl) (Table 3). In case of phosphate buffer (pH 6.8) the first order kinetics appeared to be best due to high R^2, low AIC and high MSC. The mechanism of drug release was studied by Higuchi model that showed diffusion and erosion pattern with good correlation coefficient (R^2=0.90).

The diffusion mechanism was further confirmed by 'n' value of Korsemeyer-Peppas model which was found to be less than 0.5 that further authenticated diffusion-controlled drug release. These findings agree with literature (Yarraguntla et al., 2016; Ahmed et al., 2019; Hanif et al., 2018). Thus, in pH 6.8 phosphate buffer, F1 followed first order release that was regulated by diffusion and erosion mechanism.

In pH 1.2 (0.1 N HCl) Weibull model might be responsible for drug release kinetics because of high R^2, low AIC and high value of MSC while drug release mechanism was diffusion controlled derived from n value ($n \leq 0.45$) of Korsemeyer-Peppas model. The Weibull model explained two geometric features such as α (intercept with vertical axis) and β (shape of curve). Here the shape of release curve is said to be exponential as β =1 ensuring case II transport mechanism in which drug releases through diffusion coupled with erosion from polymer matrix (Heredia et al., 2022).

Xi'an Shiyou Daxue Xuebao (Ziran Kexue Ban)/
Journal of Xi'an Shiyou University, Natural Sciences Edition
ISSN: 1673-064X
E-Publication: Online Open Access
Vol: 67 Issue 04 | 2024
DOI: 10.5281/zenodo.11063869

Table 3: Drug release Kinetic modelling of optimized formulation (F1)

F.C.	ZERO ORDER F=k0*t				FIRST ORDER F=100*[1-Exp(-k1*t)]				HIGUCHI F=kH*t^0.5				HIXON CROWELL F=100*[1-(1-kHC*t)^3]				KORSEMEYER-PEPPAS F=kKP*t^n				WEIBULL F=100*{1-Exp[-((t-Ti)^β)/α]}			
	PARAMETERS																							
	R^2 Adj	k0	AIC	MSC	R^2 Adj	k1	AIC	MSC	R^2 Adj	kH	AIC	MSC	R^2 Adj	kHC	AIC	MSC	R^2 Adj	kKP, n	AIC	MSC	R^2 Adj	α, β, Ti	AIC	MSC
F1*	0.43	0.404	78.55	0.34	0.98	0.013	48.79	3.64	0.90	6.04	63.27	2.03	0.95	0.004	55.75	2.87	0.89	8.25, 0.44	64.36	1.91	0.98	33.62, 0.81, 4.033	49.59	3.55
F1**	-1.95	0.219	72.1	-1.3	-1.19	0.003	69.92	-1.01	0.19	3.35	60.42	-0.01	-1.42	0.001	70.32	-1.11	0.89	13..6, 0.22	43.43	1.88	0.91	5815, 1.0, -185.9	41.88	2.05

Where F.C. = Formulation code, F1= Optimized formulation *(pH 6.8 Phosphate buffer), **(pH 1.2 HCl), R^2adj.=R^2 adjusted, k0= zero order rate constant, k1= first order rate constant, kH=Higuchi release rate constant, kHC= Hixson–Crowell release rate constant, kKP= constant refers to the geometric and structural characteristics of the device and "n" is the release exponent representing mechanism of drug release, β=shape of release curve, α= scale parameter identifies time scale of the process of dissolution.

Xi'an Shiyou Daxue Xuebao (Ziran Kexue Ban)/
Journal of Xi'an Shiyou University, Natural Sciences Edition
ISSN: 1673-064X
E-Publication: Online Open Access
Vol: 67 Issue 04 | 2024
DOI: 10.5281/zenodo.11063869

4.8. Animal study

4.8.1. *In-vivo* cytotoxicity

The optimized nanoparticle, F1 was investigated for its cell viability by screening out for 3T3 cell line. It was noted that F1 showed 6.6% inhibition, at concentration of 30µg/ml, against doxorubicin as standard (30µM) (% inhibition 96.2%; IC_{50} 0.1±0.02). These results indicated that optimized formulation, F1 was non-cytotoxic and found to be biocompatible.

4.8.2. Anti-inflammatory activity

In this study the anti-inflammatory effect of optimized nanoparticles, F1 and pure lornoxicam was measured using carrageenan induced rat paw edema method with the objective of getting low dose effect. The carrageenan caused gradual rise of paw thickness over a period of 5 hours experiment. Gross photograph taken at fifth hour of each group after edema induction indicated the effect of treatment with F1 and pure lornoxicam in comparison to control (Figure 10). A dose dependent decrease in paw thickness noticed in treatment with F1 (0.3mg/kg) and pure lornoxicam (0.1 and 1mg/kg) from third hour significantly (Table 4 and Figure 11). In the first two-hour study the anti-inflammatory effect decreased significantly compared to the previous time point which indicates the first phase of inflammation (release of histamine, kinin and serotonin), owed to injection trauma mainly. All doses of F1 and pure lornoxicam produced more significant ($p<0.005$) % inhibition of edema in second inflammatory phase (release of prostaglandin). The anti-inflammatory effect of F1 (51.69%; $p<0.005$) on paw edema was higher than that of pure lornoxicam (43.11%; $p<0.005$) for the same dose (0.1 mg/kg, orally) at the same time. Maximum anti-inflammatory effect was observed by F1 at 0.3mg/kg up to 80.28%; ($p<0.005$) which was far greater than pure lornoxicam (66.98%; $p<0.005$) at 1mg/kg (Table 4 and Figure 11). The IC_{50} value (50% inhibitory concentration for edema) at fifth hour for F1 and pure drug was calculated as 0.06mg/kg and 0.29mg/kg respectively.

The results of present study can be correlated and found more effective than previous study of Helmy et al., (2017) who formulated lornoxicam loaded mixed polymeric micelles and obtained more anti-inflammatory effects at 1.3mg/kg than its free form. As lornoxicam is nonselective COX (cyclooxygenase) inhibitor thereby decreases prostaglandin synthesis due to inhibition of COX enzyme hence resulted in anti-inflammatory effect. It can be concluded from the results that F1 showed better efficiency than pure drug. It corresponds to the solubility enhancement of lornoxicam through polymeric nanoparticle formulation which probably increases its bioavailability and resulted in statistically significant results in reduced dose (0.3mg/kg) as compared to previous study (Helmy et al., 2017). Chitosan also capable of anti-inflammatory and analgesic properties (Subbiah et al., 2021) therefore when combined with lornoxicam in its nanoparticulate form produced more pronounced synergistic anti-inflammatory effects as evident from the present work.

Xi'an Shiyou Daxue Xuebao (Ziran Kexue Ban)/
Journal of Xi'an Shiyou University, Natural Sciences Edition
ISSN: 1673-064X
E-Publication: Online Open Access
Vol: 67 Issue 04 | 2024
DOI: 10.5281/zenodo.11063869

Table 4: Anti-inflammatory effects of pure lornoxicam and F1 at various doses in carrageenan induced rat paw edema model

Treatments	Dose (mg/kg)	Time points						
		0 h	0.5 h	1 h	2 h	3 h	4 h	5 h
F1	0.01	Thickness of paw (mm±SEM)						
		3.93±0.1^{ns,a,1}	4.21±0.05 ^{ns,a,2} (28.25%)	4.7±0.08 ^{ns,a,b,3} (15.08%)	4.9±0.04^{ns,a,b,c,3,4} (13.74%)	5.08±0.05^{*,b,c,4} (22.23%)	4.97±0.08 ^{***,b,c,4} (38.82%)	4.93±0.08^{***,b,c,4} (42.55%)
	0.1	3.95±0.06 ^{ns,a,1}	4.19±0.03^{*,a,1} (39.88%)	4.63±0.06^{*,a,b,2} (25.54%)	4.83±0.06^{*,b,c,2} (22.47%)	4.84±0.11^{***,c,d,2} (40.45%)	4.77±0.11^{***,c,d,2} (51.69%)	4.69±0.12^{***,c,d,2} (57.44%)
	0.3	4.02±0.03 ^{ns,a,1}	4.25±0.04 ^{ns,a,2} (44.59%)	4.59±0.07^{*,a,b,3,4} (37.59%)	4.74±0.05^{***,c,4} (36.8%)	4.66±0.1^{***,d,4} (57.62%)	4.58±0.1 ^{***,d,3,4} (67.49%)	4.37±0.1^{***,e,2,3} (80.28%)
Pure Lornoxicam	0.01	4.03±0.02 ^{ns,a,1}	4.3±0.03^{ns,a,2} (32.13%)	4.71±0.08 ^{ns,a,b,3} (25.8%)	5±0.07 ^{ns,a,b,4} (14.32%)	5.22±0.05^{ns,a,b,5} (20.37%)	5.16±0.06^{***,b,4,5} (33.68%)	5.11±0.06^{***,b,4,5} (38.36%)
	0.1	3.93±0.06 ^{ns,a,1}	4.19±0.04^{*,a,2} (35.18%)	4.6±0.09^{*,a,b,3} (26.88%)	4.92±0.08 ^{ns,a,b,c,4} (12.56%)	4.86±0.08 ^{***,c,d,3,4} (37.84%)	4.91±0.13 ^{***,b,c,4} (43.11%)	4.79±0.13^{***,c,d,3,4} (50.44%)
	1	3.99±0.03 ^{ns,a,1}	4.23±0.05 ^{ns,a,2} (40.72%)	4.56±0.07^{**,b,3} (37.59%)	4.87±0.09^{*,a,b,c,4} (22.67%)	4.84±0.1*** ^{,c,d,4} (43.79%)	4.8±0.08^{***,c,d,4} (52.73%)	4.57±0.04^{***,d,e,3} (66.98%)
Control		3.91±0.12	4.32±0.05	4.83±0.09	5.05±0.07	5.41±0.13	5.63±0.13	5.66±0.11

Where; thickness of paw in mm represented Mean±SEM of n = 9 animals of 3 independent experiments in control and treated groups, % inhibition of edema presented in brackets at different time points; h=hour, $^{*}p < 0.05$, $^{**}p < 0.01$ and $^{***}p < 0.005$ = significant difference, ns=non-significant difference with respect to control, superscripts showing similar letters or numerals represented non-significant difference while dissimilar letters or numerals represented significant difference within column or within rows as per Duncan test respectively.

Xi'an Shiyou Daxue Xuebao (Ziran Kexue Ban)/
Journal of Xi'an Shiyou University, Natural Sciences Edition
ISSN: 1673-064X
E-Publication: Online Open Access
Vol: 67 Issue 04 | 2024
DOI: 10.5281/zenodo.11063869

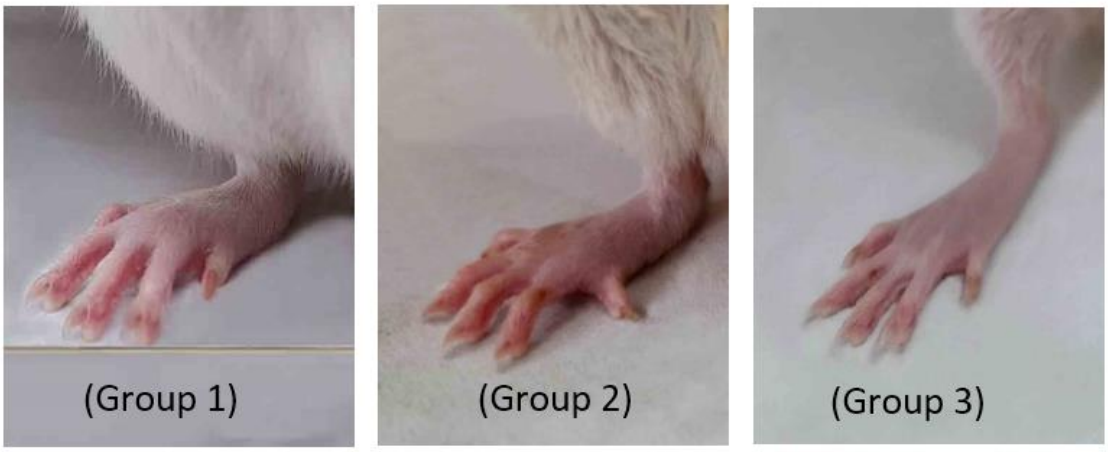

Figure 10: Gross photograph of edema in right hind paw of rats at 5th hour in three groups after carrageenan injection (n=9 rats of 3 independent experiments per group). Group 1 represents control pretreated with 10% DMSO. Group 2 represents treatment with pure lornoxicam (1mg/kg). Group 3 represents treatment with optimized nanoparticle, F1 (0.3mg/kg) respectively.

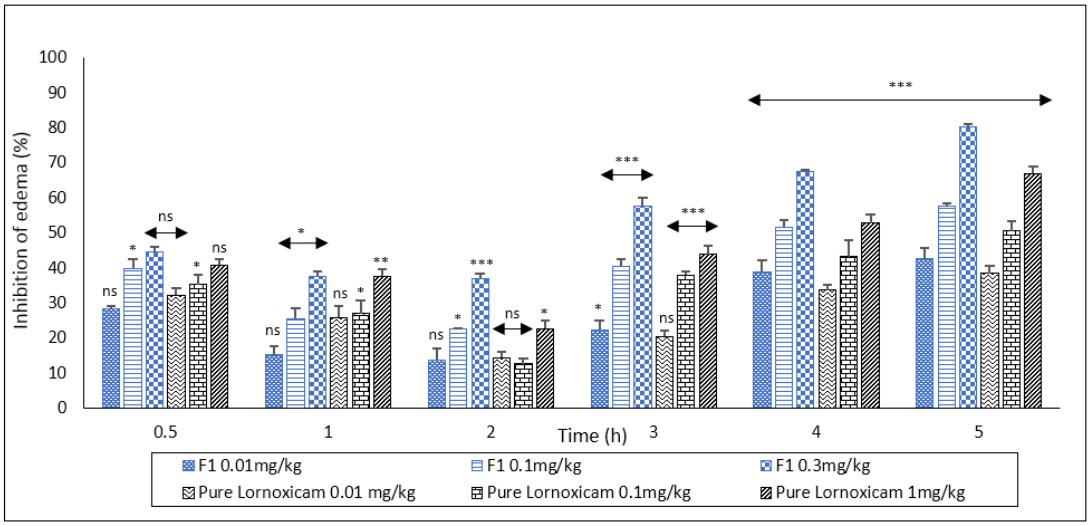

Figure 11: Percent inhibition of edema produced by optimized formulation F1 and pure lornoxicam at various doses and time points.

Where; each bar represents Mean ±SEM of inhibition of edema (%) for n=9 rats/dose of 3 independent experiments, h= hour, ns represents non-significant difference, asterisks represent significant difference; $^{*}p < 0.05$, $^{**}p < 0.01$ and $^{***}p < 0.005$ with respect to control.

Xi'an Shiyou Daxue Xuebao (Ziran Kexue Ban)/
Journal of Xi'an Shiyou University, Natural Sciences Edition
ISSN: 1673-064X
E-Publication: Online Open Access
Vol: 67 Issue 04 | 2024
DOI: 10.5281/zenodo.11063869

5. CONCLUSIONS

Polymeric nanoparticles of lornoxicam was successfully fabricated using chitosan and soluplus® through anti-solvent precipitation method. All nanoparticulate formulations showed superior characteristic features in nanodimensions with enhanced solubility, % drug release, semi crystalline, stable structure and potent anti-inflammatory properties at low dose in rats comparatively to pure lornoxicam. Chitosan and soluplus® appeared to be a promising combination that successfully increased solubility of lornoxicam in nanoparticles with excellent anti-inflammatory effects. *In-vivo* human studies of lornoxicam nanoparticles, its role in arthritis model are recommended for future researches.

Acknowledgment

Authors would like to acknowledge Sindh HEC Indigenous Scholarship (2020-21) through student financial aid office, University of Karachi for providing funds to conduct current research study and Department of Chemistry, University of Karachi to provide facility of FTIR analysis.

Conflict of Interest

The authors have no conflict of interest.

References

1) Agarwal, M., Agarwal, M. K., Shrivastav, N., Pandey, S., Das, R. and Gaur, P. 2018. Preparation of chitosan nanoparticles and their in-vitro characterization. Int. J. life-sci. sci. res. 4(2): 1713–1720.

2) Ahmed, L., Atif, R., Eldeen, T. S., Yahya, I., Omara, A. and Eltayeb, M. 2019. Study the using of nanoparticles as drug delivery system based on mathematical models for controlled release. IJLTEMAS. 8:52-56.

3) Almotairi, N., Mahrous, G. M., Al-Suwayeh, S. and Kazi, M. 2022. Design and optimization of lornoxicam dispersible tablets using Quality by Design (QbD) Approach. Pharmaceuticals. 15(12): 1463.

4) Ambrus, R., Alshweiat, A., Szabó-Révész, P., Bartos, C. and Csóka, I. 2022. Smartcrystals for efficient dissolution of poorly water-soluble meloxicam. Pharmaceutics. 14(2): 245.

5) Aslam, S., Jahan, N., Rehman, K. and Asi, M. R. 2020. Development of sodium lauryl sulphate stabilized nanosuspension of Coriandrum sativum to enhance its oral bioavailability. J. Drug Deliv. Sci. Technol. 60. 101957.

6) Carvalho, A. C. S., Zangaro, G. A. C., Fernandes, R. P., Ekawa, B., Nascimento, A. L. C. S., Silva, B. F., Ashton, G. P., Parkes, G.M.B., Lonashiro, M. and Caires, F. J. 2019. Lornoxicam drug—A new study of thermal degradation under oxidative and pyrolysis conditions using the thermoanalytical techniques, DRX and LC-MS/MS. Thermochim. Acta. 680: 178353.

7) Engelhardt, G., Homma, D., Schlegel, K., Utzmann, R. and Schnitzler, C. 1995. Anti-inflammatory, analgesic, antipyretic and related properties of meloxicam, a new non-steroidal anti-inflammatory agent with favourable gastrointestinal tolerance. Inflamm. Res. 44(10): 423–433.

8) França, M. T., Pereira, R. N., Riekes, M. K., Pinto, J. M. O. and Stulzer, H. K. 2018. Investigation of novel supersaturating drug delivery systems of chlorthalidone: The use of polymer-surfactant complex as an effective carrier in solid dispersions. Eur. J. Pharm. Sci. 111: 142-152.

ISSN: 1673-064X
E-Publication: Online Open Access
Vol: 67 Issue 04 | 2024
DOI: 10.5281/zenodo.11063869

9) Güncüm, E., Işıklan, N., Anlaş, C., Ünal, N., Bulut, E. and Bakırel, T. 2018. Development and characterization of polymeric-based nanoparticles for sustained release of amoxicillin–an antimicrobial drug. Artif. Cells Nanomed. Biotechnol. 46(sup2): 964-973.

10) Hanif, A. M., Sial, A. A., Ali, H., Zafar, F., Baig, M. T., Bushra, R., Khan, M. A, Nawab, A., Mustapha, O and Shafique, S. 2018. Dexibuprofen: Statistical assessment of drug release kinetics and investigative quality perspective. Pak. J. Pharm. Sci. 31(Supp5): 2157-2162.

11) Hassani, N. A., Abdouss, M., and Faghihi, S. 2014. Synthesis and evaluation of PEG-O-chitosan nanoparticles for delivery of poor water-soluble drugs: Ibuprofen. Mater. Sci. Eng. C. 41: 91-99.

12) Heredia, N. S., Vizuete, K., Flores-Calero, M., Pazmiño V, K., Pilaquinga, F., Kumar, B. and Debut, A. 2022. Comparative statistical analysis of the release kinetics models for nanoprecipitated drug delivery systems based on poly (lactic-co-glycolic acid). PLoS One, 17(3): e0264825.

13) Helmy, H. S., El-Sahar, A. E., Sayed, R. H., Shamma, R. N., Salama, A. H., and Elbaz, E. M. 2017. Therapeutic effects of lornoxicam-loaded nanomicellar formula in experimental models of rheumatoid arthritis. Int. J. Nanomedicine. 7015-7023.

14) Jin, I. S., Jo, M. J., Park, C. W., Chung, Y. B., Kim, J. S., and Shin, D. H. 2020. Physicochemical, pharmacokinetic, and toxicity evaluation of soluplus® polymeric micelles encapsulating fenbendazole. Pharmaceutics. 12(10): 1000.

15) Khan, M. T., Uddin, Z., Javed, M. A., Shah, N., Bashir, H., Shaikh, A. J., Rajoka, M. S. R., Amirzada, M. I., and Asad, M. H. H. Bin. 2022. PEGylated protamine letrozole nanoparticles: A promising strategy to combat human breast cancer via MCF-7 cell lines. BioMed Res. Int. 1–7.

16) Lan, Y., Ali, S. and Langley, N. 2010. Characterization of Soluplus® by FTIR and Raman Spectroscopy. Results and Disscusion. CRS 2010 (Annual Conference).

17) Li, L. S., Chiroma, S. M., Hashim, T., Adam, S. K., Moklas, M. A. M., Yusuf, Z. and Rahman, S. A. 2020. Antioxidant and anti-inflammatory properties of Erythroxylum cuneatum alkaloid leaf extract. Heliyon. 6(6).

18) Li, P., Wang, Y., Peng, Z., She, F. and Kong, L. 2011. Development of chitosan nanoparticles as drug delivery systems for 5-fluorouracil and leucovorin blends. Carbohydr. Polym. 85(3): 698–704.

19) Mirtajaddini, S. A., Najafi, M. F., Yazdi, S. A. V., and Oskuee, R. K. 2021. Preparation of chitosan nanoparticles as a capable carrier for antigen delivery and antibody production. Iran. J. Biotechnol. *19*(4), e2871.

20) Modi, A., and Tayade, P. 2006. Enhancement of dissolution profile by solid dispersion (kneading) technique. AAPS PharmSciTech. 7, E87-E92.

21) Mosmann, T. 1983. Rapid colorimetric assay for cellular growth and survival: application to proliferation and cytotoxicity assays. J. Immunol. Methods. *65*(1-2): 55-63.

22) Naik, J., Rajput, R., and Singh, M. K. 2021. Development and evaluation of ibuprofen loaded hydrophilic biocompatible polymeric nanoparticles for the taste masking and solubility enhancement. Bionanoscience. 11(1): 21–31.

23) Rahim, H., Sadiq, A., Khan, S., Amin, F., Ullah, R., Shahat, A. A. and Mahmood, H. M. 2019. Fabrication and characterization of glimepiride nanosuspension by ultrasonication-assisted precipitation for improvement of oral bioavailability and in vitro α-glucosidase inhibition. Int. J. Nanomedicine. 6287-6296.

ISSN: 1673-064X
E-Publication: Online Open Access
Vol: 67 Issue 04 | 2024
DOI: 10.5281/zenodo.11063869

24) Salarbashi, D., Tafaghodi, M., Fathi, M., Aboutorabzade, S. M. and Sabbagh, F. 2021. Development of curcumin-loaded Prunus armeniaca gum nanoparticles: Synthesis, characterization, control release behavior, and evaluation of anticancer and antimicrobial properties. Food Sci. Nutr. 9(11): 6109-6119.

25) Shariare, M. H., Altamimi, M. A., Marzan, A. L., Tabassum, R., Jahan, B., Reza, H. M., Rahman, M., Ahsan, G. U. and Kazi, M. 2019. In vitro dissolution and bioavailability study of furosemide nanosuspension prepared using design of experiment (DoE). Saudi Pharm. J. 27(1): 96–105.

26) Sharma, M., Sharma, R., Jain, D. K. and Saraf, A. 2019. Enhancement of oral bioavailability of poorly water-soluble carvedilol by chitosan nanoparticles: Optimization and pharmacokinetic study. Int. J. Biol. Macromol. 135: 246-260.

27) Subbiah, L., Palanisamy, S., Thamizhmurasu, S., Mathew Joseph, A. B., Thangavelu, P., Ganeshan, M. and Thimiri Govinda Raj, D. B. 2021. Development of meloxicam-chitosan magnetic nanoconjugates for targeting rheumatoid arthritis joints: Pharmaceutical characterization and preclinical assessment on murine models. J. Magn. Magn. Mater. 523: 167571.

28) Sunita, S. S. and Avinash, H. H. 2014. Preparation and evaluation of nanosuspensions for enhancing the dissolution of lornoxicam by antisolvent precipitation technique. Indo. Am. J. Pharm. Res. 4: 398-405.

29) Sutradhar, K. B., Khatun, S. and Luna, I. P. 2013. Increasing possibilities of nanosuspension. J. Nanotechnol. 2013. 346581.

30) Twal, S., Jaber, N., Al-Remawi, M., Hamad, I., Al-Akayleh, F. and Alshaer, W. 2024. Dual stimuli-responsive polymeric nanoparticles combining soluplus and chitosan for enhanced breast cancer targeting. RSC Adv. 14(5): 3070-3084.

31) Vengala, P.A. and Vanamala, R.U. 2018. Nanocrystal technology as a tool for improving dissolution of poorly soluble drug, lornoxicam. Int. J. Appl. Pharm. 10: 162-168.

32) Yang, H., Teng, F., Wang, P., Tian, B., Lin, X., Hu, X., Zhang, L., Zhang, Y. and Tang, X. 2014. Investigation of a nanosuspension stabilized by Soluplus® to improve bioavailability. Int. J. Pharm. 477(1-2): 88-95.

33) Yarraguntla, S. R., Enturi, V. Viadana, R. and Bommala, S. 2016. Formulation and evaluation of lornoxicam nanocrystals with different stabilizers at different concentrations. Asian J. Pharm. 10(3): 198-207.

34) Yegireddy, M., Nadoor, P., Rao, S., Hanumanthu, P.B., Rajashekaraiah, R., Ramachandrappa, S. C., Halemani, G. M., Mannem, S., Prasad, T. N. V. K. V. and Ubaradka, S. 2022. Chitosan encapsulated meloxicam nanoparticles for sustained drug delivery applications: Preparation, characterization, and pharmacokinetics in wistar rats. Molecules. 27(21): 7312.

35) Yuan, Z., Ye, Y., Gao, F., Yuan, H., Lan, M., Lou, K., and Wang, W. 2013. Chitosan-graft-β-cyclodextrin nanoparticles as a carrier for controlled drug release. Int. J. Pharm. 446(1-2): 191-198.